

FORWARD – BACKWARD AZIMUTHAL CORRELATION IN HIGH ENERGY NUCLEUS-NUCLEUS INTERACTIONS

SWARNAPRATIM BHATTACHARYYA¹, MARIA HAIDUC², ALINA TANIA NEAGU²,
ELENA FIRU²

¹ Department of Physics, New Alipore College, L Block, New Alipore, Kolkata 700053, India
E-mail: swarna_pratim@yahoo.com

² Institute of Space Science, Bucharest, Romania

Received October 27, 2014

Abstract. Forward-backward azimuthal correlation among the pions has been investigated in $^{32}\text{S} - \text{AgBr}$ interactions at 4.5 AGeV/c, $^{28}\text{Si} - \text{AgBr}$ interactions at 4.5 AGeV/c, $^{16}\text{O} - \text{AgBr}$ interactions at 4.5 AGeV/c and $^{22}\text{Ne} - \text{AgBr}$ interactions at 4.1 AGeV/c. For all the interactions mentioned above, prominent pion-pion correlations are found to occur in the azimuthal angle space. Our analysis further reveals that the forward-backward multiplicity correlation strength increases for all the interactions as the angular gap or angular interval ($\Delta\phi$) between the forward and backward azimuthal zones increases. A set of data generated by a Monte Carlo code based on the Ultra Relativistic Quantum Molecular Dynamics (UrQMD) model has been employed to compare the experimental results. The UrQMD model has failed to replicate the experimental findings.

Key words: forward-backward multiplicity correlation, azimuthal angle space.

1. INTRODUCTION

The study of nucleus-nucleus interactions at high energies has been a subject of major interest to the theoretical and experimental physicists. The nucleus-nucleus interaction can provide valuable information on the spatiotemporal development of multiparticle production process, which is one of the prime interests in view of recent developments of quantum chromodynamics (QCD). Matter described by QCD, the theory of strong interactions, may undergo phase transitions when its temperature and chemical potential is varied. QCD at finite temperature is studied in the laboratory by colliding heavy ions at varying beam energies [1].

The study of large density fluctuations in high-energy interactions received much attention due to its potential to provide a handful of information about the

dynamics of multiparticle production process [2–3]. The inclusive single particle cross section calculation provided the first clear indications of the presence of saturation effects. However, more recently, the study of angular correlations between two particles has become the area of most interest [4–14]. Two particle correlations are in fact more sensitive than inclusive production to distinguish between model predictions. The study of correlations among the particles produced in different rapidity regions may provide important information to understand the multiparticle production dynamics. Correlation studies are important for the knowledge about the late stages of interactions. It plays a fundamental role in extracting first information on the particle production mechanism.

It is believed that one of the signatures of a hot, dense medium expected to appear in most central high-energy collisions of heavy ions, will be modification of properties of jets – highly collimated streams of particles, originating from hard scatterings of partons and therefore produced early in a collision – because of their interactions with that medium. Unfortunately direct reconstruction of jets in the presence of a large background of such events is an extremely a challenging task. One possible answer to this problem is the study of azimuthal correlation. In recent times the studies of azimuthal correlation has thus gained interest among the physicists [15–21]. Two particle azimuthal correlations represent a powerful tool for characterizing the transitional region between dilute and saturated partonic systems. Studies of azimuthal correlation in terms of collective flow, azimuthal anisotropy and elliptic flow have become important research topics in recent years [22–26]. Since the first data were taken at RHIC, one of the most important experimental signatures of the QGP has been the azimuthal anisotropy in correlations between detected particles. In particular, the large value of the so-called ‘elliptic flow’ observable, indicating strong collective behavior of the collision system, has been one of the most important and most studied measurements. It provided one of the strongest pieces of evidence leading to the conclusion that a strongly coupled, low-viscosity, QGP medium is created in these collisions. Elliptic flow refers to a second Fourier component of the azimuthal distribution of emitted particles. When two identical nuclei collide at a finite impact parameter, the overlap region is an oblong shape in the transverse plane. In the standard picture, the system comes to an approximate local equilibrium and expands according to (viscous) hydrodynamics. The elliptic asymmetry in the initial state is transformed during the collective expansion into an asymmetry in the final momentum distribution of the detected particles. The efficiency of this transformation is sensitive to medium properties such as viscosity.

In the context of correlation study, it is to mention that the study of forward-backward pseudo-rapidity correlation in the nucleus–nucleus interactions at relativistic and ultra-relativistic energies has received considerable experimental and theoretical attention over the last decade [27–34]. The study of fluctuations and

correlations in forward and backward pseudo-rapidity windows has been suggested as a useful means of revealing the mechanism of particle production. The experimental study of forward-backward pseudo-rapidity correlations becomes a hot topic in relativistic heavy ion collisions with the availability of high multiplicity event-by-event measurements at the CERN-SPS and BNL-RHIC experiments. In comparison to that, so far, no attempts have been to study the correlation among the produced particles in the forward and backward azimuthal region in high-energy nucleus-nucleus interactions.

The study of forward-backward azimuthal correlation could be interesting and physics output extracted from such an analysis may be helpful in revealing the dynamics of particle production mechanism. The goal of our present study is to search for forward-backward azimuthal correlation among the produced pions in high-energy nucleus-nucleus collisions. In this paper, therefore, we have presented a detailed picture of forward-backward azimuthal correlation among the pions produced in $^{32}\text{S} - \text{AgBr}$ interactions at 4.5 AGeV/c, $^{28}\text{Si} - \text{AgBr}$ interactions at 4.5 AGeV/c, $^{16}\text{O} - \text{AgBr}$ interactions at 4.5 AGeV/c and $^{22}\text{Ne} - \text{AgBr}$ interactions at 4.1 AGeV/c. The experimental results have also been compared with the results obtained from the analysis of event sample generated by the UrQMD model in azimuthal angle (ϕ) space for all the interactions.

2. EXPERIMENTAL DETAILS

The present analysis is based on the interactions of ^{32}S projectiles at an incident momentum of 4.5 AGeV/c, ^{28}Si projectile at 4.5 AGeV/c, ^{16}O projectile at 4.5 AGeV/c and ^{22}Ne projectile at the incident momentum of 4.1 AGeV/c with AgBr as target present in nuclear emulsion. The data were obtained by exposing the stacks of NIKFI-BR2 emulsion pellicles of dimension 20 cm \times 10 cm \times 600 μ m horizontally to 4.5 AGeV/c ^{32}S , ^{28}Si , ^{16}O beams and to 4.1 AGeV/c ^{22}Ne beam at Dubna Synchrophasotron. The intensity of the irradiation was $10^3 - 10^4$ particles/cm². The beam diameter was about 1 cm. Along the track double scanning was carried out fast in the forward direction and slowly in the backward direction. ‘‘Along the track’’ scanning method gives reliable event samples because of its high detection efficiency [35–37]. Scanning was performed in 100 \times magnification. Two independent observers scanned each plate so that biases in detection, counting and measurements can be minimized. This process helps us to obtain a scanning efficiency more than 99%. Charge evaluation by delta rays and/or blob counting were carried out on usual scanning microscopes and geometrical measurements were done on the special microscope KSM

(*Kernspurmessmikroskop*) made by Karl Zeiss Jena. The final measurements were carried out with the help of an oil-immersion objective of $750 \times$ magnification.

Events were chosen according to the criteria mentioned below:

- a) The incident beam track would have to lie within 3° from direction of the main beam in the pellicle. This criterion ascertains that the real projectile beam has been selected for the analysis.
- b) Events showing interactions within $20 \mu\text{m}$ from the top and bottom surface of the pellicle were rejected. Rejection of such events reduces the losses of tracks and minimizes the uncertainties in the measurements of emission and azimuthal angles.
- c) All the primary beam tracks were followed in the backward direction to ensure that the events chosen did not include interactions from the secondary tracks of the other interactions.

According to the terminology of nuclear emulsion, particles emitted from an interaction (called an event or a star) are classified into four categories, namely the shower particles, the grey particles, the black particles and the projectile fragments [38]. Characteristics of these particles are given below.

Shower particles. The tracks of particles having ionization I less or equal to $1.4I_0$ are called shower tracks. I_0 is the minimum ionization of a singly charged particle. Shower particles are mostly pions (about more than 90%) with a small admixture of kaons and hyperons (less than 10%). Nuclear emulsion track detector cannot distinguish among pions, other mesons and hyperons. Estimation of percentage of kaons, hyperons or other mesons along with pions in nuclear emulsion can be done by applying any event generator [39]. In one of our papers [39], we have applied the Ultra Relativistic Quantum Molecular Dynamics (UrQMD) model to calculate the percentage of kaons, hyperons and other mesons along with pions in nuclear emulsion for $^{32}\text{S}-\text{AgBr}$ interactions at $4.5 \text{ AGeV}/c$, $^{28}\text{Si}-\text{AgBr}$ interactions at $4.5 \text{ AGeV}/c$, $^{16}\text{O}-\text{AgBr}$ interactions at $4.5 \text{ AGeV}/c$ and $^{22}\text{Ne}-\text{AgBr}$ interactions at $4.1 \text{ AGeV}/c$. A brief discussion on UrQMD model will be presented later. In Table 1, we have shown the percentage of occurrences of pions, kaons ϕ – mesons, Λ – hyperons and η mesons produced at (4.1–4.5) AGeV/c . From Table 1 it can be noted that in $^{32}\text{S}-\text{AgBr}$, $^{28}\text{Si}-\text{AgBr}$, $^{16}\text{O}-\text{AgBr}$ and $^{22}\text{Ne}-\text{AgBr}$ interactions at (4.1–4.5) AGeV/c , $(91.19 \pm 0.08) \%$ to $(92.40 \pm 0.10) \%$ of the shower particles are pions and $(7.60 \pm 0.09) \%$ to $(8.81 \pm 0.09) \%$ of the shower particles are kaons ϕ – mesons, Λ – hyperons and η mesons. These shower particles are produced in a forward cone. The velocities of these particles are greater than $0.7c$, where c is the velocity of light in free space. Because of such a high velocity, these particles are not generally confined within the emulsion pellicle. Energies of these shower particles lie in the GeV range. To avoid contamination between the single-charged produced

particles and the spectator projectile protons, shower tracks falling within the Fermi cone were excluded from our analysis. The Fermi cone is characterized by a semi-vertex angle θ_f where $\theta_f = P_{Fermi} / P_{inc}$. Here P_{inc} is the incident projectile momentum per nucleon measured in GeV/c and P_{Fermi} is the Fermi momentum in GeV/c of the nucleons of the projectile fragments. The value of P_{Fermi} can be calculated based on Fermi gas model of the nucleus and the numerical value of P_{Fermi} comes out to be 0.21 GeV/c [36, 40].

Grey particles. Grey particles are mainly fast target recoil protons with energies up to 400 MeV. They have ionization $1.4 I_0 \leq I < 10 I_0$. Ranges of these particles are greater than 3 mm in the emulsion medium. These grey particles have the velocities lying between $0.3c$ and $0.7c$.

Black particles. Black particles consist of both singly and multiply charged fragments. They are fragments of various elements like carbon, lithium, beryllium etc with ionization greater or equal to $10I_0$. These black particles have the maximum ionizing power. They are less energetic and consequently they are short ranged. In the emulsion medium, ranges of black particles are less than 3 mm. The velocities of the black particles are less than $0.3c$. In emulsion experiments, it is very difficult to measure the charges of the target fragments. Therefore, it is not possible to identify the exact nucleus.

Projectile fragments. The projectile fragments are the spectator parts of the incident projectile nucleus that do not directly participate in an interaction. They are emitted within a very narrow extremely forward cone whose semi-vertex angle ($\theta_f = P_{Fermi} / P_{inc}$) is determined by the Fermi momenta of the nucleons present in the nucleus. Having almost the same energy or momentum per nucleon as the incident projectile, these fragments exhibit uniform ionization over a long range and suffer negligible scattering.

Nuclear emulsion medium consists of variety of nuclei like H, C, N, O, Ag and Br. The interaction of the projectile beam can happen with any of these nuclei. As already mentioned that in emulsion experiment, it is very difficult to measure the charges of the fragments emitted from the target and hence exact identification of the target is not possible. However, we can divide the major constituent elements present in the emulsion into three broad target groups namely hydrogen (H), light nuclei (CNO) and heavy nuclei (*AgBr*). So in the experiments with the nuclear emulsion track detectors, interactions can be classified depending on the collisions of projectiles with different kinds of target *e.g.*, hydrogen (H), light nuclei (CNO) and heavy nuclei (*AgBr*) present in the emulsion medium. The black and grey tracks together in an event are known as heavy tracks and are denoted by N_h . Number of heavy tracks in an interaction is an important parameter because target identification is done depending on the total number of heavy tracks (N_h).

Usually events with $N_h \leq 1$ have occurred as a result of collisions between the hydrogen present in emulsion and the projectile beam. This is because when hydrogen nucleus is the target, on collision with the projectile beam, fragmentation of the target will occur and the only proton present in the hydrogen nucleus will be emitted. Obviously, in this case number of heavy tracks cannot exceed one. Events with $2 \leq N_h \leq 8$ are due to collisions of the projectile beam with the light nuclei (CNO). In case of interactions of the projectile beam with the light nuclei (CNO), it is evident that maximum number of heavy tracks cannot exceed eight. This corresponds to the largest charge of the light nucleus-the oxygen nucleus. Events with $N_h > 8$ are due to collisions of the projectile beam with the heavy target (*AgBr*). It can easily be understood that when $N_h > 8$, it can be ascertained that the projectile has collided with such a target whose atomic number is greater than eight. It is clear that in this case, the target group cannot be the light target group (CNO). It will be the heavy target group (*AgBr*). In this way by counting the number of heavy tracks, one can determine the target group.

In this method of target identification, the separation of events for *AgBr* target is quite accurate in the sample with $N_h > 8$ but in $2 \leq N_h \leq 8$ there is an admixture of CNO events and events generated from peripheral collisions between the projectile and *AgBr* target. The aim of this paper is to study the non-peripheral interactions of the projectile beam with the heavy target (*AgBr*) group. So we have only considered $N_h > 8$. We are not interested to study the projectile-hydrogen or projectile-CNO interactions. Therefore, we have not considered those events having $N_h \leq 1$. Thus, we have excluded the events occurring due to the collision between the hydrogen present in emulsion and the projectile beam. It has been mentioned that we have not considered those events, which have $2 \leq N_h \leq 8$. We have thus excluded the CNO events and excluded any possibility of events occurring due to peripheral collisions with the *AgBr* target also.

In the light of the above method of target identification, we have selected 434 events of $^{32}\text{S}-\text{AgBr}$, 514 events of $^{28}\text{Si}-\text{AgBr}$ and 1057 events of $^{16}\text{O}-\text{AgBr}$ interactions at 4.5 AGeV/c and 1584 events of $^{22}\text{Ne}-\text{AgBr}$ interactions at 4.1 AGeV/c [39]. We have carried out our analysis in the azimuthal angle space (ϕ) for the shower particles. The average multiplicities of shower tracks (mostly pions), has been presented in Table 2 for all the four interactions. The azimuthal angle (ϕ) for each shower track was measured by applying simple coordinate geometry after taking the readings of the coordinates of the interaction point (X_0, Y_0, Z_0), coordinates (X_1, Y_1, Z_1) at the end of the linear portion each secondary track and coordinates (X_i, Y_i, Z_i) of a point on the incident beam.

Nuclear emulsion detectors offer a good angular resolution. This advantage can be exploited when the distribution of particles in a small phase space region is investigated. It has been pointed out in [41], when single particle distributions are

measured, inefficiency of a detector is not a serious obstacle. A number of undetected particles should be estimated and the single particle distribution can be corrected easily. In the case of correlation measurements, the effect of lost particles on the measured correlation depends on how the lost particles are correlated with the detected ones. Since the correlation is a priori not known, it is unclear how the observed correlation should be corrected. For this reason, the correlation measurements should be performed where the detector efficiency is almost perfect. Nuclear emulsion track detector is best suited for this purpose as they are capable of registering all the produced or emitted particles in the 4π geometry.

3. METHOD OF ANALYSIS

In order to study forward-backward azimuthal correlation, the azimuthal angle space has to be divided into two distinct zones, one is called the forward azimuthal zone and the other one is the backward azimuthal zone. There should be an angular gap between the two zones. Throughout our analysis, we shall call this angular gap as azimuthal angle interval or azimuthal angle separation $\Delta\phi$. Forward-backward azimuthal correlations are characterized by the forward-backward correlation strength, b [29]. Forward-backward azimuthal correlations are investigated by calculating the multiplicities of the produced charged particles on an event-by-event basis in the forward and backward azimuthal zones. For each event, the multiplicity of charged particles falling in the forward azimuthal zone is compared with that of the backward azimuthal zone. Let N_f be the multiplicity of the produced charged particles in the forward azimuthal zone and N_b be the multiplicity of the produced charged particles in the backward azimuthal zone. In terms of N_f and N_b , in azimuthal angle space, the forward-backward correlation strength b can be defined in the same manner as defined in [27, 29]

$$b = \frac{\langle N_f N_b \rangle - \langle N_f \rangle \langle N_b \rangle}{\langle N_f^2 \rangle - \langle N_f \rangle^2}. \quad (1)$$

The quantities within angular brackets are event-averaged values. Putting $\langle N_f N_b \rangle = \langle N_f \rangle \langle N_b \rangle$ in equation (1) we get $b = 0$. When $b = 0$, it may be said that the charged particles have been produced randomly and independently signifying uncorrelated particle emission. On the other hand if $N_b = N_f$ in every event, we should have $b = 1$ *i.e.* occurrence of maximum correlation during the particle production.

4. ANALYSIS AND RESULTS

To study the forward-backward multiplicity correlation in the azimuthal angle space, we have constructed two azimuthal zones, one from 0 to ϕ_1 and another from ϕ_2 to ϕ_3 . The first azimuthal zone is referred as the forward azimuthal angle zone and the second one is the backward azimuthal angle zone.

The difference between ϕ_1 and ϕ_2 is the azimuthal angular interval $\Delta\phi$. For the present analysis, we have divided the azimuthal zone into three pairs of forward-backward zones as illustrated below.

Initially the forward azimuthal zone has been considered from 0° to 65° and the backward azimuthal zone has been selected from 70° to 130° . So that the angular difference $\Delta\phi$ between the two zones comes out to be 5° . Next we decrease the forward azimuthal range by 5° keeping the backward range unaltered so that the angular difference becomes $\Delta\phi = 10^\circ$. Here the forward azimuthal zone is from 0° to 60° and the backward azimuthal zone is from 70° to 130° . Following the same procedure another azimuthal angular difference $\Delta\phi = 15^\circ$ is created. In this case, forward azimuthal zone is from 0° to 55° and the backward azimuthal zone is from 70° to 130° .

We have calculated the values of $N_f, N_b, \langle N_f \rangle, \langle N_b \rangle$ and $\langle N_f N_b \rangle$ for $^{32}\text{S} - \text{AgBr}$, $^{28}\text{Si} - \text{AgBr}$, $^{16}\text{O} - \text{AgBr}$ and $^{22}\text{Ne} - \text{AgBr}$ interactions for the three sets of forward-backward zone with $\Delta\phi = 5^\circ, 10^\circ$ and 15° . Using relation (1) we have computed the values of forward-backward correlation coefficient (b) for all the four interactions stated above and for each values of the azimuthal angular interval $\Delta\phi$. The values of the correlation coefficient and the values of $\Delta\phi$ have been presented in Table 3 for $^{32}\text{S} - \text{AgBr}$, $^{28}\text{Si} - \text{AgBr}$, $^{16}\text{O} - \text{AgBr}$ and $^{22}\text{Ne} - \text{AgBr}$ interactions. From the table it is clear that the values of the forward-backward correlation coefficient b are significantly greater than zero for all the interactions and for all the angular separation $\Delta\phi$. Non-zero values of correlation coefficient speak in favor of the presence of forward-backward multiplicity correlations among the pions in the azimuthal angle space in high-energy nucleus-nucleus interactions at Dubna energy. From Table 3 it can also be noted that the values of forward-backward correlation coefficient (b) increase with the increase

in $\Delta\phi$. Moreover as the higher values of b indicate stronger correlation, we may infer that correlations among the pions are strongest for $^{32}\text{S} - \text{AgBr}$ interactions.

The variations of forward-backward correlation strength b as a function of the azimuthal angle interval $\Delta\phi$ are depicted in Fig. 1a for $^{32}\text{S} - \text{AgBr}$ interactions at 4.5 AGeV/c, in Fig. 1b for $^{28}\text{Si} - \text{AgBr}$ interactions at 4.5 AGeV/c, in Fig. 1c for $^{16}\text{O} - \text{AgBr}$ interactions at 4.5 AGeV/c and in Fig. 1d for $^{22}\text{Ne} - \text{AgBr}$ interactions at 4.1 AGeV/c. Errors shown in all the figures are purely statistical. We have calculated the statistical error according to the formula given in [42].

For the proper understanding of the physical significance of this correlation, it is necessary to compare the experimental results with the results obtained from an existing event generator. The Ultra Relativistic Quantum Molecular Dynamics (UrQMD) model [43] may be a good candidate for this purpose. Therefore, the analysis of forward-backward azimuthal correlation has also been performed by analyzing events generated by the UrQMD model for $^{32}\text{S} - \text{AgBr}$, $^{28}\text{Si} - \text{AgBr}$, $^{16}\text{O} - \text{AgBr}$ and $^{22}\text{Ne} - \text{AgBr}$ interactions. UrQMD model is a microscopic transport theory based on the covariant propagation of all the hadrons on the classical trajectories in combination with stochastic binary scattering, color string formation and resonance decay. It represents a Monte Carlo solution of a large set of coupled partial integro-differential equations for the time evolution of various phase space densities.

The main ingredients of the model are the cross sections of binary reactions, the two-body potentials and decay widths of resonances. This model can be used in the entire available range of energies from the Bevalac region to RHIC. For more details about this model, readers are requested to consult [44].

We have generated a large sample of events using the UrQMD code for $^{32}\text{S} - \text{AgBr}$, $^{28}\text{Si} - \text{AgBr}$, $^{16}\text{O} - \text{AgBr}$ and $^{22}\text{Ne} - \text{AgBr}$ interactions. Taking Ag and Br nuclei as target, events were generated separately for each target. According to the proportional abundance of Ag and Br nuclei present in the nuclear emulsion, the generated events were mixed with each other in order to get the desired UrQMD data sample. We have also calculated the average multiplicities of the shower tracks (mostly pions) for all the interactions in case of the UrQMD data sample. Average multiplicities of the shower tracks in case of UrQMD data sample have been presented in Table 2 along with the average multiplicity values of shower particles for the experimental events. Table 2 shows that the average multiplicities of the shower tracks for the UrQMD events are comparable with those of the experimental values for all the interactions.

The analysis of multiplicity correlation in forward and backward azimuthal zones has been repeated for the data sample generated by the UrQMD model in case of $^{32}\text{S} - \text{AgBr}$, $^{28}\text{Si} - \text{AgBr}$, $^{16}\text{O} - \text{AgBr}$ and $^{22}\text{Ne} - \text{AgBr}$ interactions. We have divided the total azimuthal zone into three same pairs of forward-backward zone as in the case of experimental study and calculated the correlation coefficient b for each values of $\Delta\phi$ and for each interaction. The values of the forward-backward correlation coefficients (b) have been tabulated in Table 3 for all the interactions along with the corresponding experimental values. From Table 3 it is seen that the correlation coefficients in case of UrQMD data sample are less than those of their experimental counterparts. The correlation coefficient values for the UrQMD data sample are found to increase with the increase of $\Delta\phi$. Our analysis with the UrQMD data sample signifies that the UrQMD model cannot reproduce the experimental results. It may therefore be concluded that the experimental data reveals the true dynamical signal. In order to have a clear comparison, the variations of forward-backward correlation strength b as a function of the azimuthal angle interval $\Delta\phi$ for the UrQMD generated data are presented in Fig. 1a for $^{32}\text{S} - \text{AgBr}$ interactions, in Fig. 1b for $^{28}\text{Si} - \text{AgBr}$ interactions, in Fig. 1c for $^{16}\text{O} - \text{AgBr}$ interactions and in Fig. 1d for $^{22}\text{Ne} - \text{AgBr}$ interactions respectively along with the experimental values.

Table 1

The percentage of π - mesons, kaons, ϕ - mesons, Λ - hyperons and η mesons obtained from UrQMD model for $^{32}\text{S} - \text{AgBr}$ interactions at 4.5 AGeV/c, $^{28}\text{Si} - \text{AgBr}$ interactions at 4.5 AGeV/c, $^{16}\text{O} - \text{AgBr}$ interactions at 4.5 AGeV/c and $^{22}\text{Ne} - \text{AgBr}$ interactions at 4.1 AGeV/c

Particle Produced	Interactions			
	$^{32}\text{S} - \text{AgBr}$ 4.5 AGeV/c	$^{28}\text{Si} - \text{AgBr}$ 4.5 AGeV/c	$^{16}\text{O} - \text{AgBr}$ 4.5 AGeV/c	$^{22}\text{Ne} - \text{AgBr}$ 4.1 AGeV/c
% of π - mesons produced	(91.44±.13)%	(91.78±.11)%	(92.40±.10)%	(91.19±.08)%
% of Kaons produced	(4.01±.07)%	(3.80±.06)%	(3.43±.05)%	(4.86±.04)%
% of ϕ - mesons produced	(1.96±.04)%	(1.85±.03)%	(1.58±.01)%	(1.59±.01)%
% of Λ - hyperons produced	(1.49±.04)%	(1.44±.03)%	(1.45±.02)%	(1.36±.03)%
% of η mesons produced	(1.08±.02)%	(1.11±.01)%	(1.11±.01)%	(0.99±.01)%

Table 2

The average multiplicities of the shower particles (mostly pions) for all the interactions in case of the experimental and the UrQMD data

Interactions	Average multiplicity of shower tracks	
	Experimental data	UrQMD data
$^{32}\text{S} - \text{AgBr}$ (4.5 AGeV/c)	28.04 ± 0.14	30.83 ± 0.17
$^{28}\text{Si} - \text{AgBr}$ (4.5 AGeV/c)	23.62 ± 0.21	27.55 ± 0.22
$^{16}\text{O} - \text{AgBr}$ (4.5 AGeV/c)	18.05 ± 0.22	17.79 ± 0.21
$^{22}\text{Ne} - \text{AgBr}$ (4.1 AGeV/c)	20.96 ± 0.12	20.92 ± 0.16

Table 3

The forward-backward correlation coefficient b for different $\Delta\phi$ values in case of experimental and UrQMD generated data for $^{32}\text{S} - \text{AgBr}$ interactions at 4.5 AGeV/c, $^{28}\text{Si} - \text{AgBr}$ interactions at 4.5 AGeV/c, $^{16}\text{O} - \text{AgBr}$ interactions at 4.5 AGeV/c and for $^{22}\text{Ne} - \text{AgBr}$ interactions at 4.1 AGeV/c

Interactions	$\Delta\phi$ in degree	correlation coefficient b	
		Experimental	UrQMD
$^{32}\text{S} - \text{AgBr}$ interactions at 4.5 AGeV/c	5	$.456 \pm .010$	$.162 \pm .006$
	10	$.483 \pm .013$	$.172 \pm .007$
	15	$.515 \pm .014$	$.183 \pm .009$
$^{28}\text{Si} - \text{AgBr}$ interactions at 4.5 AGeV/c.	5	$.376 \pm .015$	$.179 \pm .008$
	10	$.381 \pm .017$	$.189 \pm .009$
	15	$.397 \pm .020$	$.199 \pm .010$
$^{16}\text{O} - \text{AgBr}$ interactions at 4.5 AGeV/c	5	$.347 \pm .015$	$.179 \pm .007$
	10	$.358 \pm .017$	$.190 \pm .009$
	15	$.362 \pm .018$	$.202 \pm .010$
$^{22}\text{Ne} - \text{AgBr}$ interactions at 4.1 AGeV/c	5	$.450 \pm .013$	$.179 \pm .005$
	10	$.472 \pm .016$	$.190 \pm .007$
	15	$.492 \pm .017$	$.199 \pm .008$

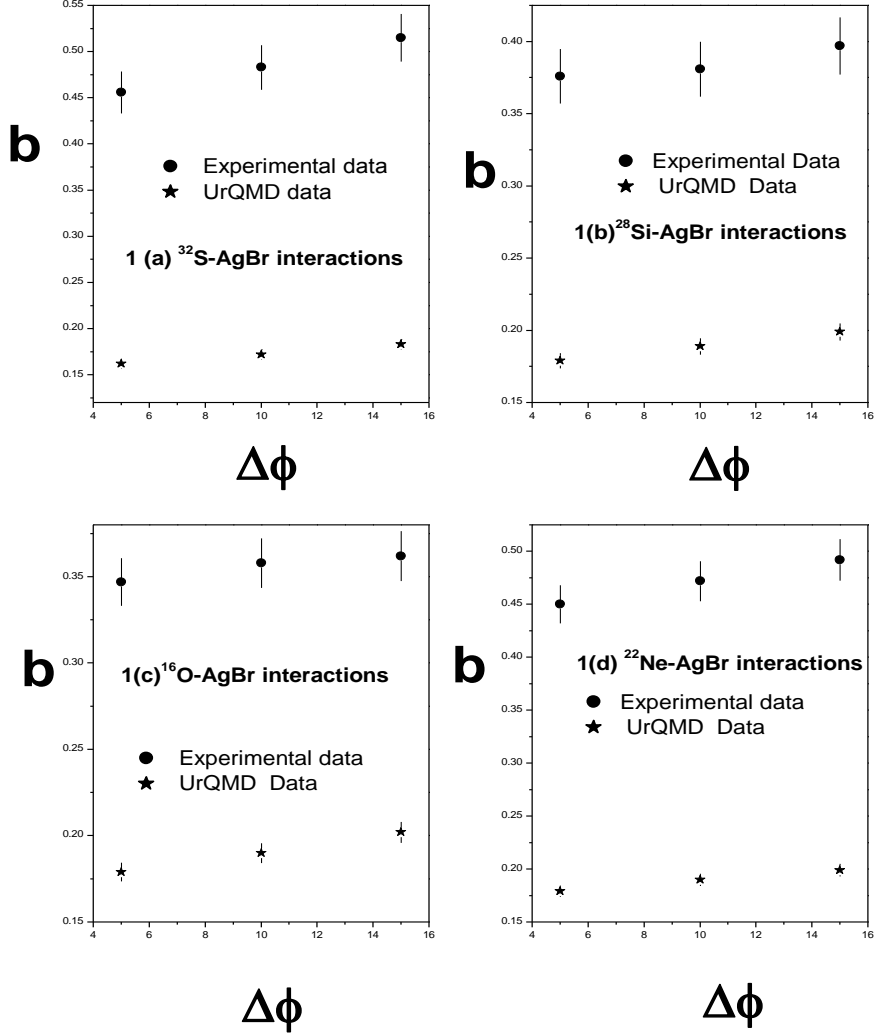


Fig. 1 – The variation of the correlation coefficient b against the angular difference between forward and backward azimuthal zone $\Delta\phi$ in case of a) $^{32}\text{S}-\text{AgBr}$ interactions at 4.5 AGeV/c; b) $^{28}\text{Si}-\text{AgBr}$ interactions at 4.5 AGeV/c; c) $^{16}\text{O}-\text{AgBr}$ interactions at 4.5 AGeV/c; d) $^{22}\text{Ne}-\text{AgBr}$ interactions at 4.1 AGeV/c for both the experimental and UrQMD data.

5. DISCUSSION ON SYSTEMATIC ERRORS

Before going to the conclusion of our analysis, it would be relevant to present a discussion on systematic errors of the data. Detailed analysis on

systematic errors for the same data set has been presented in our earlier publication [39]. From our previous paper, we find that one of the sources of systematic errors in emulsion plate can arise from the scanning and measurement procedure. It has been mentioned earlier that the technique adopted in order to find all the interactions was “Along the track” scanning technique. “Along the track” scanning procedure helps us to obtain a scanning efficiency of more than 99%. Therefore, the contributions to the systematic errors arising from the scanning and measurement procedure are less than 1%.

Systematic errors may also be introduced due to the presence of background tracks in nuclear emulsion detector. The background tracks can arise due to the decay of radioactive contamination, such as thorium present both in emulsion and in their glass backings [45]. Some of such tracks may also be caused by the cosmic radiations during the time of exposure. But to confuse a background track with the tracks coming from an event, the track has to originate from the interaction vertex – the chance of which is only accidental. Moreover, the volume occupied by all interaction vertices in an emulsion plate is negligibly small with respect to the total volume of the plate. Keeping these points in mind, the chance of a mix-up between tracks originating from an event, with the tracks caused by background radiations are very very small.

To the readers the issue of background contamination in emulsion detector due to production of electron pair tracks may be an important issue to be addressed. However, the electron pair tracks produced through γ – conversion do not emanate from the interaction vertex, but are produced at a distance from the vertex after traveling through certain radiation lengths. In order to eliminate all the possible backgrounds due to γ overlap (where a γ from a π^0 decay converts into e^+e^- pair) close to shower tracks near vertex, special care was taken to exclude such e^+e^- pairs from the primary shower tracks while performing angular measurements. Usually all shower tracks in the forward direction were followed more than 100–200 μm from the interaction vertex for angular measurement. The tracks due to e^+e^- pair can be easily recognized from the grain density measurement, which is initially much larger than the grain density of a single charged pions or proton track. It may also be mentioned that the tracks of an electron and positron when followed downstream in nuclear emulsion showed considerable amount of Coulomb scattering as compared to the energetic charged pions. Such e^+e^- pairs were eliminated from the data. Therefore, any possibility of systematic errors arising because of background tracks is negligibly small in emulsion detectors.

6. CONCLUSION

From our present analysis, it can be concluded that prominent forward-backward pion-pion correlations are found to survive in the azimuthal angle space for $^{32}\text{S} - \text{AgBr}$ interactions at 4.5 AGeV/c, $^{28}\text{Si} - \text{AgBr}$ interactions at 4.5 AGeV/c, $^{16}\text{O} - \text{AgBr}$ interactions at 4.5 AGeV/c and $^{22}\text{Ne} - \text{AgBr}$ interactions at 4.1 AGeV/c. The correlation coefficient increases with the increase of azimuthal angle interval $\Delta\phi$ for all the four interactions. Experimental results have also been compared with the UrQMD model predictions. UrQMD model cannot reproduce the main qualitative features of azimuthal correlation. The observed discrepancy of the obtained results with the UrQMD data sample is quite interesting. This discrepancy establishes that the observed correlations are not merely of statistical reason. Rather the correlation may be interpreted because of dynamical fluctuation present in the multi particle production mechanism.

To the best of our knowledge, this is for the first time, azimuthal correlations have been analyzed in such a way using forward and backward multiplicity correlation technique. The observed behavior of forward-backward azimuthal correlation may be viewed as an experimental fact. In terms of the physics message, there are many possible sources of particle azimuthal correlations. To arrive at some definite conclusion about the sources of forward-backward azimuthal correlation, more higher energy data analysis is extremely important.

Acknowledgements. This work was supported by a project of the Romanian National Authority for Scientific Research, UEFISCDI, project number PN-II-ID-PCE-2011-3-0978, Contract No.: 69/05.10.2011.

The authors are grateful to Prof. Pavel Zarubin, JINR, Dubna, Russia for providing them the required emulsion data. The corresponding author Dr. Swarnapratim Bhattacharyya will like to thank Prof. Adam Bzdak of RIKEN BNL Research Center, Brookhaven National Laboratory, Upton, NY 11973, USA and Prof. Subhasis Chattopadhyay of VECC, India for some useful discussions. Dr. Bhattacharyya also acknowledges Prof. Dipak Ghosh, Department of Physics, Jadavpur University and Prof. Argha Deb, Department of Physics, Jadavpur University, for their inspiration in the preparation of this manuscript.

REFERENCES

1. S. Gupta *et al.*, Science **332**, 1525 (2011).
2. L. Adamczyk *et al.* (STAR Collaboration), Phy. Rev. Lett. **112**, 032302 (2014).
3. M.M. Aggarwal *et al.* (STAR Collaboration), Phy Rev Lett **105**, 022302 (2010).
4. S. S. Adler *et al.*, Phys. Rev. C **76**, 034903 (2007).
5. J. Adams *et al.* (STAR Collaboration), Phys. Rev. C **75**, 034901 (2007).
6. E. Braidot, Nucl. Phys. A **854**, 168 (2011).
7. P.K. Netrakanti (for the STAR collaboration), Nucl. Phys. A **854**, 102 (2011).

8. J. G. Ulery, Acta Physica Polonica B Proceedings, Supplement **1**, 629 (2008).
9. P. Bozek and W. Broniowski, Phys. Rev. Lett. **109**, 062301 (2012).
10. S. Gavin and G. Moschelli, Phys. Rev. Lett. **85**, 014905 (2012).
11. A. Bzdak, arXiv: 1108.0882v3 [hep-ph], 2 May 2012.
12. H. Bialkowska, Acta Phy. Pol. B **42**, 1359 (2011).
13. M.S. Nilsson, *et al.*, Phys. Rev D **84**, 054006 (2011).
14. T. Todoroki, arXiv:1209.0044v2[nucl-ex], 3 Oct. 2012.
15. M. Szuba (STAR Collaboration), Ind. Jour. of Phys. **85**, 1057 (2011).
16. S. Chartrchyan *et al.*, CMS collaboration, arxiv 1210.5482v2 [nucl-ex], 22 Oct. 2012.
17. Wei Li, Mod. Phy Lett A **27**, 1230018 (2012).
18. J.L. Albacete and C. Marquet, Phy. Rev. Lett. **105**, 162301 (2010).
19. A.H. Tang (STAR Collaboration), Jour. of Phys. G **31**, S35 (2005).
20. B. Abelev *et al.* (ALICE Collaboration), Phys. Lett. B **719**, 29 (2013).
21. Xuan Li (For STAR Collaboration), arXiv:1212.1686v1[nucl-ex], 7 Dec 2012.
22. L.Adamczyk *et al.* (STAR Collaboration), arXiv: 1301.2348v1 [nucl-ex], 10 Jan 2013.
23. M. Csanad *et al.*, Euro. Phys. Jour. A **38**, 363 (2008).
24. H. Van Hess *et al.*, Phy. Rev. C **84**, 054906 (2011).
25. U. Heinz and R. Snellings, arXiv: 1301.2826v1, 13 Jan 2013.
26. X. Zhang and J. Liao, arXiv: 1210.1245v1[nucl-ex], 3 Oct. 2012.
27. M. Skoby, STAR Collaboration, Nucl. Phys. A **854**, 113 (2011).
28. T. Lappi, Nucl. Phys A **854**, 117 (2011).
29. B. K. Srivastava (for the STAR collaboration), Journ. of Phys. G. **35**, 104140 and references there in (2008).
30. C. Pajares, Nucl. Phys. A **854**, 125 (2011).
31. A. Bzdak, Phys. Rev. C **85**, 051901(R) and references there in (2012).
32. A. Bzdak, Acta Phys. Pol. B **41**, 2471 (2010).
33. Na Li *et al.*, Jour. of Phy. G **39**, 115105 (2012).
34. A.K. Dash, D.P. Mahapatra and B. Mohanty, Int. Jour. of Mod. Phy. A **27**, 1250079 (2012).
35. M.I. Adamovich *et al.*, EMU01 Collaboration, Jour. of Phys. G **22**, 1469 (1996).
36. M.I. Adamovich *et al.*, EMU01 Collaboration, Phys. Lett. B **227**, 285 (1989).
37. M.I. Adamovich *et al.*, EMU01 Collaboration, Phys. Lett. B **223**, 262 (1989).
38. C.F. Powell, P.H. Fowler and D.H Perkins, *The Study of the Elementary Particles by Photographic Method*, Oxford Pergamon Press, pp. 450–464 and references therein, 1959.
39. S. Bhattacharyya, M. Haiduc, A.T. Neagu and E. Firu, Journ. of Phys. G **40**, 025105 (2013); S. Bhattacharyya, M. Haiduc, A.T. Neagu and E. Firu, Phys. Lett. B **726**, 194 (2013).
40. P. Mali, A. Mukhopadhyay and G. Singh, Phys. Scripta **85**, 065202 (2012).
41. S. Mrowczynski, Acta Phy. Pol. B **40**, 1053 (2009).
42. Carsten Sogaarded, *Measurements of Forward-Backward Charged Particle Correlations with ALICE*, Thesis presented for the degree of Doctor of Philosophy (PhD) in Physics, 3rd May 2012.
43. M. Bleicher, E. Zabrodin, C. Spieles, S.A. Bass, C. Ernst, S. Soff, L. Bravina, M. Belkacem, H. Weber, H. Stocker, W. Greiner, Journ. of Phys. G. **25**, 1859 (1999).
44. S. A. Bass, M. Belkacem, M. Bleicher, M. Brandstetter, L. Bravina, C. Ernst, L. Gerland, M. Hofmann, S. Hofmann, J. Konopka, G. Mao, L. Neise, S. Soff, C. Spieles, H. Weber, L.A. Winckelmann, H. Stocker, W. Greiner, Ch. Hartnack, J. Aichelin and N. Amelin, Prog. Part. Nucl. Phys. **41**, 255 (1998).
45. A. Beiser, Rev.of. Mod. Phys. **24**, 273 (1952).